ELSEVIER

Available online at www.sciencedirect.com

SCIENCE DIRECT®

Polymer 46 (2005) 4361–4367

polymer

www.elsevier.com/locate/polymer

Conformational origin of the molecular weight dependence of the characteristic ratio of the dipole moment in poly(A-B)

Carin A. Helfer*, Wayne L. Mattice

Institute of Polymer Science, The University of Akron, Akron, OH 44325-3909, USA

Abstract

By poly(A-B) we denote a chain with repeating sequence –A-B–, such as polyoxymethylene. Here A and B stand for a single atom, e.g., –O–, or a group of atoms, e.g., $-CH_2-$. All n bond vectors are of the same length, l, as are all bond dipole moment vectors, m. The manner in which the characteristic ratio of the dipole moment, $D_n \equiv \langle \mu^2 \rangle_0 / nm^2$ approaches its asymptotic limit is related quantitatively to the behavior of subchains of various sizes in poly(A-B). Illustrative numerical calculations with rotational isomeric state (RIS) models for several polymers are consistent with the predictions. The approach of D_n to its asymptotic limit is sensitive to longer subchains than is the approach of the characteristic ratio of the end-to-end distance, $C_n \equiv \langle r^2 \rangle_0 / nl^2$, to its asymptotic limit, due to the differences in the connectivity of the bond vectors (head-to-tail) and the bond dipole moment vectors (head-to-head, tail-to-tail).

Keywords: Poly(A-B); Dipole moment vector; Asymptotic limit

1. Introduction

The mean square dipole moment, $\langle \mu^2 \rangle$, is one of the fundamental conformation-dependent physical properties of a polar macromolecule [1–4]. The RIS model is especially useful for rationalizing $\langle \mu^2 \rangle$ because this property, in contrast to the mean square end-to-end distance, $\langle r^2 \rangle$, is insensitive to the excluded volume effect in long polar polymers for which the average projection of the dipole moment vector onto the end-to-end vector, $\langle \boldsymbol{\mu} \cdot \mathbf{r} \rangle_0$, is zero in the unperturbed chain [5–8]. Nearly four decades of literature contain numerous joint experimental and RIS studies of $\langle \mu^2 \rangle_0$ for chain molecules [9–40] or RIS studies that make comparisons with experimental results published elsewhere [41–61]. Theoretical evaluations of $\langle \mu^2 \rangle_0$ have also been employed to understand the behavior of chains for which experimental results were not available [62–73].

The chain vectors $\mathbf{r}$ and $\boldsymbol{\mu}$ can be treated as a sum of vectors associated with individual bonds in the chain. The vectors are the bond vector, $\mathbf{l}$, and the bond dipole moment vector, $\mathbf{m}$. The n bond vectors are connected in a head-to-tail fashion in a linear chain. In general, some of the bonds in the chain may have a null bond dipole moment vector, as is the CH_2–CH_2 bond in polyoxyethylene, and bonds that are not in the main chain may make important contributions to $\langle \mu^2 \rangle$, as in the poly(vinyl alkyl ether)s. However, for chains of the type poly(A-B), composed of two different types of atoms that alternate in their appearance in the chain, and in the absence of polar side chains, as in polyoxymethylene (POM), the same relationship connects the $\mathbf{l}_i$ and $\mathbf{r}$, and the $\mathbf{m}_i$ and $\boldsymbol{\mu}$.

$$\mathbf{r} = \sum_{i=1}^{n} \mathbf{l}_i \tag{1}$$

$$\boldsymbol{\mu} = \sum_{i=1}^{n} \mathbf{m}_i \tag{2}$$

Every bond in the main chain has a non-zero $\mathbf{l}_i$ and a non-zero $\mathbf{m}_i$, and all n of the $\mathbf{l}_i$ are of the same length, as are all n of the $\mathbf{m}_i$. The only important difference is that the $\mathbf{l}_i$ are connected head-to-tail, and the $\mathbf{m}_i$ are connected head-to-head, tail-to-tail. Such chains typically have characteristic ratios for the end-to-end distance, C_n, that are larger than one.

$$C_n \equiv \frac{\langle r^2 \rangle_0}{nl^2} \tag{3}$$

---

* Corresponding author. Tel.: +1 330 972 6104.
E-mail address: carin@polymer.uakron.edu (C.A. Helfer).

0032-3861/$ - see front matter © 2005 Elsevier Ltd. All rights reserved.
doi:10.1016/j.polymer.2005.03.019

However, the corresponding characteristic ratio for the dipole moment, D_n, is usually less than one.

$$D_n \equiv \frac{\langle\mu^2\rangle_0}{nm^2} \tag{4}$$

Our concern here is with the manner in which D_n for poly(A-B) makes the final approach to its asymptotic limit, as represented quantitatively by the initial slope of D_n vs. $1/n$. A model-independent analytical expression for this initial slope is obtained by a method that parallels the recent treatment of the analogous property of C_n, namely the initial slope of C_n vs. $1/n$ [74]. RIS calculations are performed to illustrate how the short-range interactions in the chain affect the value of $[\mathrm{d}D_n/\mathrm{d}(1/n)]_{1/n=0}$. Some of the results are not surprising. Thus we find that $[\mathrm{d}D_n/\mathrm{d}(1/n)]_{1/n=0}$ is usually positive, in contrast with $[\mathrm{d}C_n/\mathrm{d}(1/n)]_{1/n=0}$, which is usually negative. The difference in sign is expected if $C_\infty > 1$ but $D_\infty < 1$. However, $C_\infty > 1$ does not guarantee that $[\mathrm{d}C_n/\mathrm{d}(1/n)]_{1/n=0}$ will always be negative, as documented by the case of syndiotactic poly(methyl methacrylate) [74]. A more surprising conclusion from the present work is that the value of $[\mathrm{d}D_n/\mathrm{d}(1/n)]_{1/n=0}$ can be more sensitive to the behavior of longer subchains than is the value of $[\mathrm{d}C_n/\mathrm{d}(1/n)]_{1/n=0}$, even when the absolute value of $[\mathrm{d}D_n/\mathrm{d}(1/n)]_{1/n=0}$ is two orders of magnitude smaller than the absolute value of $[\mathrm{d}C_n/\mathrm{d}(1/n)]_{1/n=0}$. This surprising conclusion follows from numerical calculations for POM and arise from the difference in the connectivity of the bond vectors, **l**, and the bond dipole moment vectors, **m**.

2. Mathematical formulation

An analytical expression for $[\mathrm{d}D_n/\mathrm{d}(1/n)]_{1/n=0}$ for poly(A-B) can be obtained from Eqs. (2) and (4), along with the assumption that the flexible homopolymer has an even number of bonds, so that its two ends are indistinguishable. The approach is perfectly analogous to the one employed recently in the investigation of $[\mathrm{d}C_n/\mathrm{d}(1/n)]_{1/n=0}$ [74]. Since all of the bond dipole moment vectors are of the same length, $\langle\mu^2\rangle$ and D_n are given by Eqs. (5) and (6), respectively.

$$\langle\mu^2\rangle = nm^2 + 2\sum_{i=1}^{n-1}\sum_{j=i+1}^{n}\langle \mathbf{m}_i\cdot\mathbf{m}_j\rangle \tag{5}$$

$$D_n = 1 + \left(\frac{2}{nm^2}\right)\sum_{i=1}^{n-1}\sum_{j=i+1}^{n}\langle \mathbf{m}_i\cdot\mathbf{m}_j\rangle_0 \tag{6}$$

Eq. (6) can also be written using a unit vector $\mathbf{v}_i$ that is parallel with $\mathbf{m}_i$, $\mathbf{v}_i \equiv \mathbf{m}_i/m_i$.

$$D_n = 1 + \left(\frac{2}{n}\right)\sum_{i=1}^{n-1}\sum_{j=i+1}^{n}\langle \mathbf{v}_i\cdot\mathbf{v}_j\rangle_0 \tag{7}$$

The analogous expression for C_n uses the unit vector, $\mathbf{u}_i$, that is parallel with $\mathbf{l}_i$, $\mathbf{u}_i \equiv \mathbf{l}_i/l_i$ [74]:

$$C_n = 1 + \left(\frac{2}{n}\right)\sum_{i=1}^{n-1}\sum_{j=i+1}^{n}\langle \mathbf{u}_i\cdot\mathbf{u}_j\rangle_0 \tag{8}$$

To facilitate the comparison of these two properties of the chain, Eq. (7) can be written in terms of the $\mathbf{u}_i$ by incorporating the difference in the connectivity of the $\mathbf{v}_i$ and the $\mathbf{u}_i$.

$$\mathbf{v}_i = (-1)^i\mathbf{u}_i \tag{9}$$

$$D_n = 1 + \left(\frac{2}{n}\right)\sum_{i=1}^{n-1}\sum_{j=i+1}^{n}(-1)^{j-i}\langle \mathbf{u}_i\cdot\mathbf{u}_j\rangle_0 \tag{10}$$

Taking n to be large enough so that it lies within the limiting region were D_n becomes linear in $1/n$, the initial slope of D_n vs. $1/n$ can be written in terms of D_n and D_{2n} [74].

$$\left[\frac{\mathrm{d}D_n}{\mathrm{d}(1/n)}\right]_{1/n=0} = \lim_{n\to\infty}[-2n(D_{2n} - D_n)] \tag{11}$$

An instructive expression for this initial slope can be obtained by separating the double sum in Eq. (10) into three parts, defined in perfect analogy to the similar separation in the recent treatment of C_n [74].

$$T_{1,2n} = \sum_{i=1}^{n}\sum_{j=n+1}^{2n}(-1)^{j-i}\langle \mathbf{u}_i\cdot\mathbf{u}_j\rangle_0 \tag{12a}$$

$$T_{2,2n} = \sum_{i=n+1}^{2n-1}\sum_{j=i+1}^{2n}(-1)^{j-i}\langle \mathbf{u}_i\cdot\mathbf{u}_j\rangle_0 \tag{12b}$$

$$T_{3,2n} = \sum_{i=1}^{n-1}\sum_{j=i+1}^{n}(-1)^{j-i}\langle \mathbf{u}_i\cdot\mathbf{u}_j\rangle_0 \tag{12c}$$

The desired expression can be written in terms of these three double sums [74].

$$\left[\frac{\mathrm{d}D_n}{\mathrm{d}(1/n)}\right]_{1/n=0} = \lim_{n\to\infty}[-2(T_{1,2n} + T_{2,2n} - T_{3,2n})] \tag{13}$$

Since we consider only homopolymers with an even number of bonds, the ends of the chain are indistinguishable, and therefore $T_{2,2n} = T_{3,2n}$.

$$\left[\frac{\mathrm{d}D_n}{\mathrm{d}(1/n)}\right]_{1/n=0} = -2T_{1,\infty} \tag{14}$$

Since $\langle \mathbf{u}_i\cdot\mathbf{u}_j\rangle_0$ for a flexible chain must approach zero as $j-i$ increases without limit, the double sum required for $T_{1,\infty}$ can be accurately evaluated by considering only those values of $\langle \mathbf{u}_i\cdot\mathbf{u}_j\rangle_0$ for which the number of individual terms is $j-i$ [74]. This fact allows the rewriting of the double sum as a single sum over $k \equiv j-i$.

$$\left[\frac{\mathrm{d}D_n}{\mathrm{d}(1/n)}\right]_{1/n=0} = -2\sum_{k=1}^{\infty}k(-1)^k\langle \mathbf{u}_i\cdot\mathbf{u}_{i+k}\rangle_0 \tag{15}$$

In Eq. (15), it is understood that bond i is sufficiently far removed from either end of the chain so that end effects do not influence the sum. The corresponding expression for C_n does not contain the factor of $(-1)^k$ [74].

$$\left[\frac{\mathrm{d}C_n}{\mathrm{d}(1/n)}\right]_{1/n=0} = -2\sum_{k=1}^{\infty} k\langle \mathbf{u}_i \cdot \mathbf{u}_{i+k}\rangle_0 \tag{16}$$

In the next section, the influence of the factor of $(-1)^k$ is illustrated by using RIS models for several chains to calculate the $\langle \mathbf{u}_i \cdot \mathbf{u}_{i+k}\rangle_0$ as well as C_n and D_n.

3. Illustrative numerical calculations

The numerical calculations use the geometry and short-range interactions reported in previously published RIS models for polydimethylsiloxane (PDMS) [41], polydimethylsilylenemethylene (PDMSM) [46], and POM [49]. The customary generator matrices were used to calculate $\langle r^2\rangle_0$ and $\langle \mu^2\rangle_0$ as a function of n [75], and the derivatives specified by the left-hand sides of Eqs. (15) and (16) were obtained from the initial slope of the appropriate characteristic ratio vs. $1/n$. The values of $\langle \mathbf{u}_i \cdot \mathbf{u}_{i+k}\rangle_0$ were calculated as the 1,1 element of the unperturbed average of the serial product of transformation matrices, $\langle \mathbf{T}_i\mathbf{T}_{i+1}\ldots\mathbf{T}_{i+k-1}\rangle_0$ [74]. The results reported here are the averages over the two possible choices of the directionality of bond i, A–B and B–A. The behavior of $\langle \mathbf{u}_i \cdot \mathbf{u}_{i+k}\rangle_0$ and $k\langle \mathbf{u}_i \cdot \mathbf{u}_{i+k}\rangle_0$ for PDMS was reported previously [74], as was the numerical result for $[\mathrm{d}C_n/\mathrm{d}(1/n)]_{1/n=0}$ [76].

Figs. 1–3 show $\langle \mathbf{u}_i \cdot \mathbf{u}_{i+k}\rangle_0$, $k\langle \mathbf{u}_i \cdot \mathbf{u}_{i+k}\rangle_0$, and $k(-1)^k \langle \mathbf{u}_i \cdot \mathbf{u}_{i+k}\rangle_0$, respectively, for POM, using a temperature of 298 K. The $\langle \mathbf{u}_i \cdot \mathbf{u}_{i+k}\rangle_0$ exhibit an oscillation superimposed on a monotonic decay. The tendency for the formation of short *gauche* helices in unperturbed POM produces the oscillations and the negative value of $\langle \mathbf{u}_i \cdot \mathbf{u}_{i+2}\rangle_0$. The underlying monotonic decay arises because $\mathbf{u}_i$ for any flexible chain must become completely decorrelated from $\mathbf{u}_{i+k}$ in the limit as $k\to\infty$. The value of $\langle \mathbf{u}_i \cdot \mathbf{u}_{i+k}\rangle_0$ falls below 0.01 when $k>42$.

Multiplication of each term in Fig. 1 by k produces the results shown in Fig. 2. The signature of the *gauche* helices is still apparent, but the decay to zero is shifted to larger values of k. The value of $k\langle \mathbf{u}_i \cdot \mathbf{u}_{i+k}\rangle_0$ does not fall below 0.01 until $k>91$. The sum on the right-hand side of Eq. (16), obtained as the area under the curve in Fig. 2, is equal to 51. The value of the right-hand side of this equation, obtained by direct calculation of C_n as a function of n, is -102. Therefore, the manner in which C_n specified by a RIS model approaches its asymptotic limit is accurately described by Eq. (16), as expected [74].

Fig. 3 shows the result when the factor $(-1)^k$ is included in each term in the sum. The first three terms are negative and the remaining terms alternate in sign. This alternation causes the area under the curve in Fig. 3 to be drastically smaller than the area under the curve in Fig. 2. The absolute value of $[\mathrm{d}D_n/\mathrm{d}(1/n)]_{1/n=0}$, from Eq. (15), is more than two orders of magnitude smaller than the value of $[\mathrm{d}C_n/\mathrm{d}(1/n)]_{1/n=0}$ from Eq. (16). It is also of the opposite sign. C_n approaches its asymptotic limit from below, but D_n approaches its limit from above.

The validity of Eqs. (15) and (16) can be illustrated by plotting the terms on the left-hand side, as obtained by direct calculation of C_n and D_n, vs. the terms on the right-hand side, as obtained from $\langle \mathbf{u}_i \cdot \mathbf{u}_{i+k}\rangle_0$. This plot is shown in Fig. 4 for data obtained from previously published RIS models for POM [49], PDMSM [46], and PDMS [41]. The solid straight line has a slope of 1 and passes through the origin. Since the points from the RIS calculations fall very close to this straight line, Eqs. (15) and (16) accurately capture the behavior of these unperturbed chains.

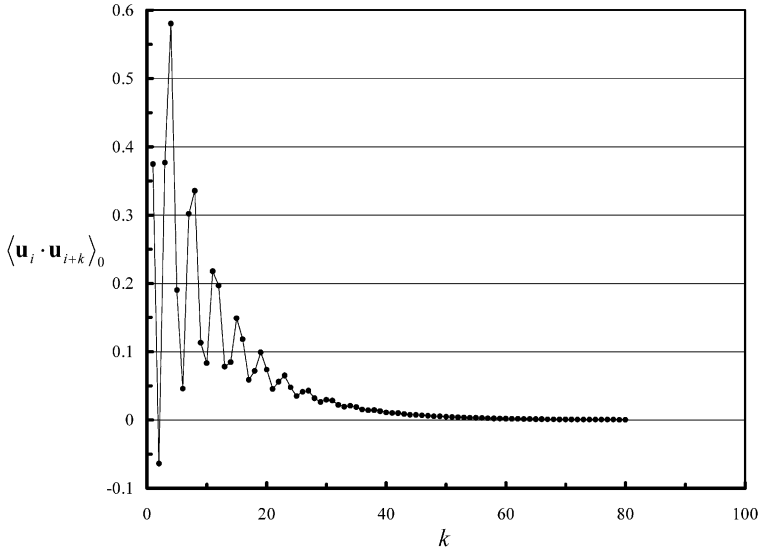

Fig. 1. The values of $\langle \mathbf{u}_i \cdot \mathbf{u}_{i+k}\rangle_0$ for POM, using the RIS model of Abe and Mark [28].

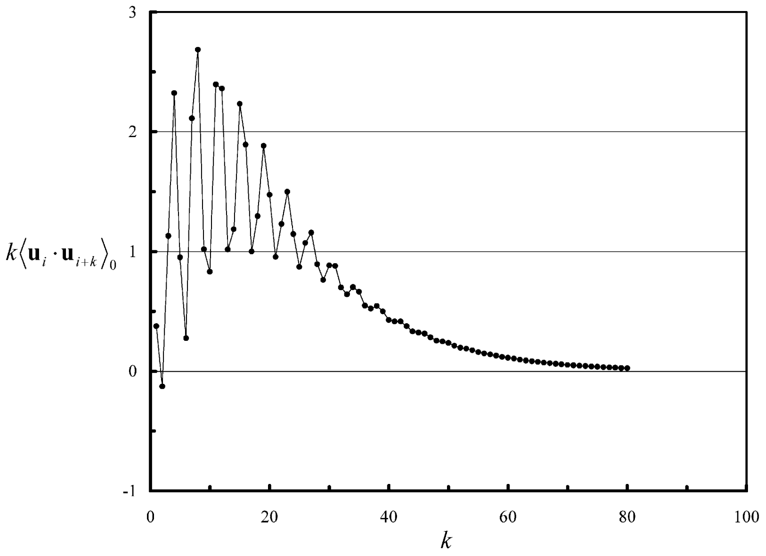

Fig. 2. The values of $k\langle \mathbf{u}_i \cdot \mathbf{u}_{i+k} \rangle_0$ for POM, using the RIS model of Abe and Mark [28].

It is of interest to compare the sizes of the subchains that contribute significantly to the values of $[\mathrm{d}C_n/\mathrm{d}(1/n)]_{1/n=0}$ and $[\mathrm{d}D_n/\mathrm{d}(1/n)]_{1/n=0}$. That comparison is made in Fig. 5, using the data for POM that is reported in Figs. 2 and 3. The vertical axis is the cumulative contribution of subchains up through the specified value of k to the pertinent summations, i.e., it is either

$$\mathrm{Cum}_C \equiv \left(-2\sum_{\kappa=1}^{\infty}\kappa\langle \mathbf{u}_i \cdot \mathbf{u}_{i+\kappa}\rangle_0\right)^{-1}\left(-2\sum_{\kappa=1}^{k}\kappa\langle \mathbf{u}_i \cdot \mathbf{u}_{i+\kappa}\rangle_0\right) \quad (17)$$

or

$$\mathrm{Cum}_D \equiv \left(-2\sum_{\kappa=1}^{\infty}\kappa(-1)^{\kappa}\langle \mathbf{u}_i \cdot \mathbf{u}_{i+\kappa}\rangle_0\right)^{-1} \times \left(-2\sum_{\kappa=1}^{k}\kappa(-1)^{\kappa}\langle \mathbf{u}_i \cdot \mathbf{u}_{i+\kappa}\rangle_0\right) \quad (18)$$

By definition, Cum_C and Cum_D have an asymptotic limit of 1 as $k \to \infty$. The former ratio, which is pertinent to $[\mathrm{d}C_n/\mathrm{d}(1/n)]_{1/n=0}$, approaches the limit monotonically from below, and is within 99% of the limit when $k > 71$. The latter ratio, which is pertinent to $[\mathrm{d}D_n/\mathrm{d}(1/n)]_{1/n=0}$, has a slower convergence and oscillates about 1. It is not reliably within 99% of the asymptotic limit until k reaches 100. Although $[\mathrm{d}D_n/\mathrm{d}(1/n)]_{1/n=0}$ is two orders of magnitude smaller in

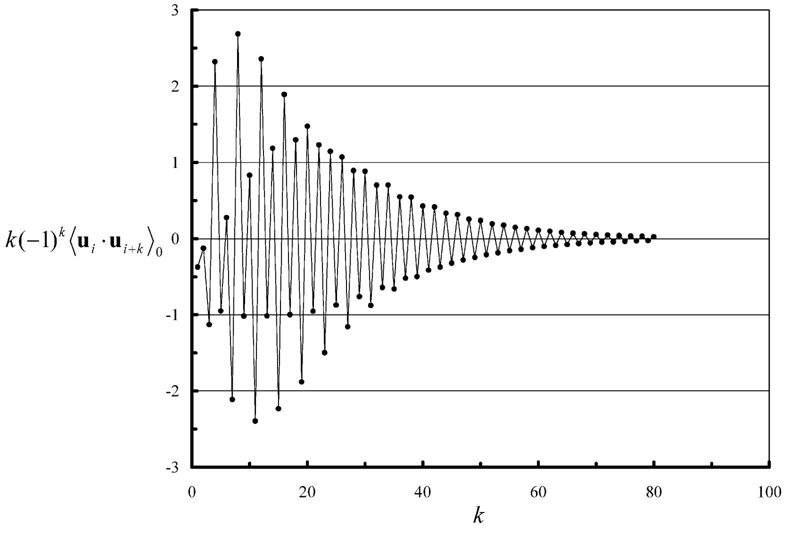

Fig. 3. The values of $k(-1)^k\langle \mathbf{u}_i \cdot \mathbf{u}_{i+k} \rangle_0$ for POM, using the RIS model of Abe and Mark [28].

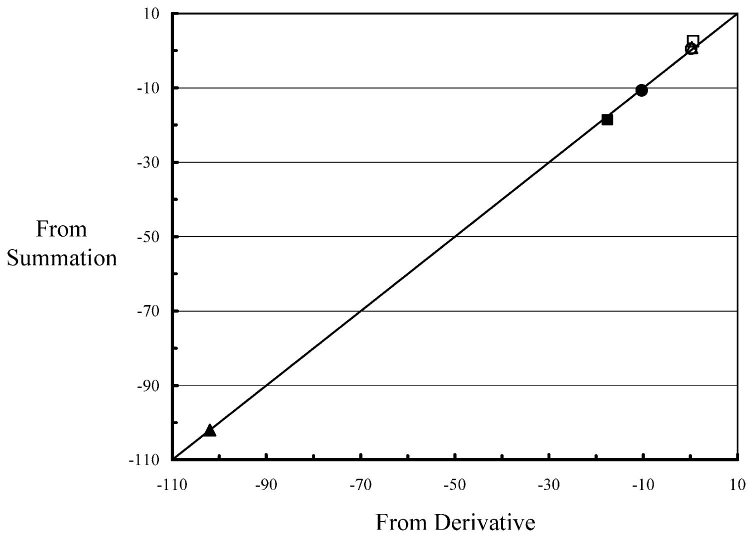

Fig. 4. Values of $[\mathrm{d}C_n/\mathrm{d}(1/n)]_{1/n=0}$ and $[\mathrm{d}D_n/\mathrm{d}(1/n)]_{1/n=0}$ obtained by direct calculation of C_n and D_n, vs. the values of $-2\Sigma k\langle \mathbf{u}_i \cdot \mathbf{u}_{i+k}\rangle_0$ and $-2\Sigma k(-1)^k\langle \mathbf{u}_i \cdot \mathbf{u}_{i+k}\rangle_0$, respectively, using RIS models for POM [49], PDMSM [46], and PDMS [41]. The straight line has a slope of one and passes through the origin. The results for $[\mathrm{d}C_n/\mathrm{d}(1/n)]_{1/n=0}$ and $-2\Sigma k\langle \mathbf{u}_i \cdot \mathbf{u}_{i+k}\rangle_0$ for PDMS are from Ref. [74]. Filled and open symbols denote $[\mathrm{d}C_n/\mathrm{d}(1/n)]_{1/n=0}$ and $[\mathrm{d}D_n/\mathrm{d}(1/n)]_{1/n=0}$, respectively. Results for POM, PDMSM, and PDMS are plotted using ▲, ●, and ■, respectively.

absolute value than $[\mathrm{d}C_n/\mathrm{d}(1/n)]_{1/n=0}$, it is sensitive to longer subchains, due to the oscillations imposed by the head-to-head, tail-to-tail connection of the bond dipole moment vectors.

4. Conclusion

The manner in which the characteristic ratio of the dipole moment for poly(A-B) approaches its asymptotic limit is accurately given by the sum of the terms $k(-1)^k\langle \mathbf{u}_i \cdot \mathbf{u}_{i+k}\rangle_0$, where $\mathbf{u}_i$ is a unit vector along bond i. The oscillations produced by the head-to-head, tail-to-tail connectivity of the bond dipole moment vectors cause the approach of D_n to its limit to be sensitive to longer subchains than is the approach of C_n to its limit.

Acknowledgements

It is a pleasure to extend our best wishes to Prof. James E. Mark on the occasion of his 70th birthday. Among his many accomplishments is the extensive characterization of the mean square dipole moments of flexible chain molecules [2, 7,10–16,19,23–25,41–43,45,46,49,51,56,62–65,68,72,73].

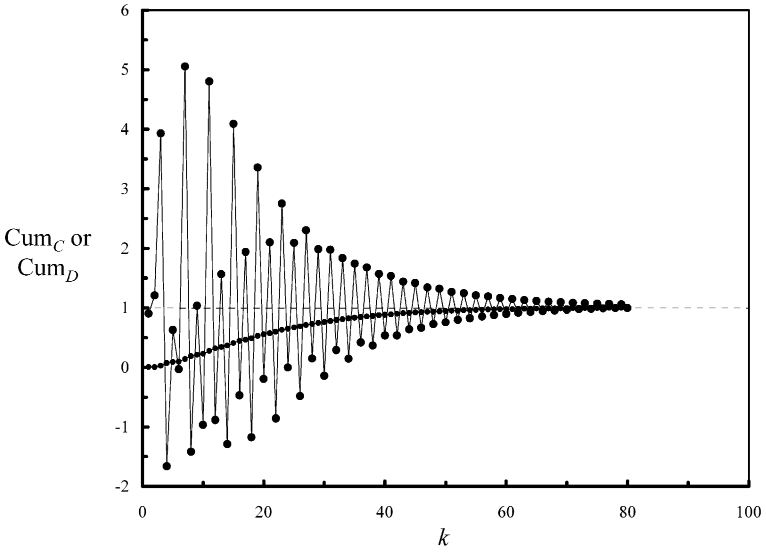

Fig. 5. Convergence of the sums on the right-hand side of Eq. (15) (monotonically increasing curve) and Eq. (16) (oscillating curve) to their limits for POM, as measured by the Cum$_C$ and Cum$_D$ defined in Eqs. (17) and (18), respectively. Both sets of data are normalized so that the asymptotic limits are 1.

This research was supported by National Science Foundation Grant DMR 0098321.

References

[1] Flory PJ. Statistical mechanics of chain molecules. New York: Wiley; 1969 p. 150–52, 155–57, 165, 168–71, 184, 188, 267, 279–80.

[2] Mark JE. Use of dipole moments to characterize configurations of chain molecules. Acc Chem Res 1974;7:218.

[3] Mattice WL, Suter UW. Conformational theory of large molecules. New York: Wiley; 1994. p. 35, 346–51.

[4] Diaz-Calleja R, Riande E. Calculation of dipole moments and correlation parameters. In: Runt JP, Fitzgerald JJ, editors. Dielectric spectroscopy of polymeric materials. Washington, DC: American Chemical Society; 1997. p. 139–73.

[5] Nagai K, Ishikawa T. Excluded-volume effect on dipole moments of polymer chains. Polym J 1971;2:416.

[6] Doi M. Excluded-volume effect on dipole moment of polar macromolecules. Polym J 1972;3:252.

[7] Liao SC, Mark JE. Effect of excluded volume on the dipole moments of chain molecules. J Chem Phys 1973;59:3825.

[8] Neuburger NA, Mattice WL. Interpretation of the mean square dipole moment of poly(A-B) by use of the mean square end-to-end distance of its didymous partner. Macromolecules 1989;22:3694.

[9] Bates TW, Stockmayer WH. Conformational properties of isolated poly(tetrafluoroethylene) chains. J Chem Phys 1966;45:2321.

[10] Bak K, Elefante G, Mark JE. Configurational properties of poly(ethylene oxide) and poly(tetramethylene oxide). J Phys Chem 1967;71:4007.

[11] Sutton C, Mark JE. Dipole moments of dimethylsiloxane oligomers and poly(dimethylsiloxane). J Chem Phys 1971;54:5011.

[12] Riande E, Mark JE. Random-coil configurations of the polyformals $[CH_2O(CH_2)_yO–]$. 1. Dipole moments of poly(1,3-dioxolane) $[CH_2\text{-}O(CH_2)_2O–]$. Macromolecules 1978;11:956.

[13] Riande E, Mark JE. Random coil configuration of polyformals. 4. Dipole moments of poly(1,3-dioxocane) and poly(1,3-dioxonane). Polymer 1979;20:1188.

[14] Riande E, Mark JE. Random coil configurations of the polyformals $[CH_2–O–(CH_2)_y–O–]$. II. Dipole moments of poly(1,3-dioxepane) $[CH_2–O–(CH_2)_4–O–]$. J Polym Sci, Polym Phys Ed 1979;17:2013.

[15] Riande E, Boileau S, Hemery P, Mark JE. An experimental study of the dipole moments of isotactic and atactic poly(propylene sulfide). Macromolecules 1979;12:702.

[16] Riande E, Boileau S, Hemery P, Mark JE. Dipole moments of poly(propylene sulfide) chains. J Chem Phys 1979;71:4206.

[17] Guest JA, Matsuo K, Stockmayer WH, Suter UW. Chain dimensions and dipole moments of poly(*tert*-butyl vinyl ketone). Macromolecules 1980;13:560.

[18] Riande E, Guzmán J, Saiz E. Random-coil configurations of alicyclic polyformals. Polymer 1981;22:465.

[19] Riande E, Garcia M, Mark JE. Random-coil configurations of the polyformals. VI. Dipole moments of the stereochemically variable polymer prepared from 4-methyl-1,3-dioxolane. J Polym Sci, Polym Phys Ed 1981;19:1739.

[20] Khanarian G, Tonelli AE. Kerr effect and dielectric study of poly(oxyethylene glycols). Macromolecules 1982;15:145.

[21] Khanarian G, Cais RE, Kometani J, Tonelli AE. Kerr effect and dielectric study of the copolymer poly(styrene-*co*-*p*-halogenated styrene). Macromolecules 1982;15:866.

[22] Tonelli AE. Conformational characteristics of poly(*N*-vinylpyrrolidinone). Polymer 1982;23:676.

[23] Riande E, Guzman J, Welsh WJ, Mark JE. Configurational characteristics of the polysulfides. 1. Dipole moments of poly(pentamethylene sulfide). Makromol Chem 1982;183:2555.

[24] Welsh WJ, Mark JE, Guzman J, Riande E. Configurational characteristics of the polysulfides. 2. Dipole moments and gauche effects in poly(1,3-dithiocane). Makromol Chem 1982;183:2565.

[25] Guzman J, Riande E, Welsh WJ, Mark JE. Configurational characteristics of the polysulfides. 3. Dipole moments of poly(trimethylene sulfide) and comparisons between some polysulfides and the corresponding polyoxides. Makromol Chem 1982;183:2573.

[26] Khanarian G, Schilling FC, Cais RE, Tonelli AE. Kerr effect and dielectric study of poly(vinyl chloride) and its oligomers. Macromolecules 1983;16:287.

[27] Riande E, Guzman J, de la Campa JG, de Abajo J. Configurational properties of polyesters with cyclohexane rings incorporated in the main chain. Macromolecules 1985;18:1583.

[28] Tonelli AE. Conformational characteristics of poly(2-vinylpyridine). Macromolecules 1985;18:2579.

[29] de la Peña JL, Riande E, Guzmán J. Random-coil configurations of alicyclic poly(thioformals). Macromolecules 1985;18:2739.

[30] Riande E, Guzmán J, Adabbo H. Conformational energies and random-coil configurations of aliphatic polyesters. Macromolecules 1986;19:2567.

[31] Tonelli AE, Valenciano M. Kerr effect and dielectric study of ethylene-vinyl chloride copolymers. Macromolecules 1986;19:2643.

[32] Riande E, de la Campa JG, Schlereth DD, de Abao J, Guzmán J. Conformational characteristics of phthalic acid based polyesters. Macromolecules 1987;20:1641.

[33] Wittwer H, Pino P, Suter UW. Dipole moments and conformational analysis of copolymer of ethylene and carbon monoxide. Macromolecules 1988;21:1262.

[34] Saiz E, Horta A, Gargallo L, Hernández-Fuentes I, Radíc D. Dipole moment and conformational analysis of itaconate polymers. Macromolecules 1988;21:1736.

[35] Riande E, Guzmán J, de Abajo J. Influence of the acid residue on the polarity of cycloaliphatic polyesters. Macromolecules 1989;22:4026.

[36] Saiz E, Riande E, San Román J, Madruga EL. Dielectric and conformational properties of phenyl and chlorophenyl esters of poly(acrylic acid). Macromolecules 1990;23:785.

[37] Saiz E, Riande E, San Román J, Madruga EL. Dipole moments and conformational properties of low molecular weight analogues of acrylate polymes with mesogenic side groups. Macromolecules 1990;23:3491.

[38] Kuntman A, Bahar I, Baysal BM. Conformational characteristics of poly(ethyl methacrylate). Dipole moment measurements and calculations. Macromolecules 1990;23:4959.

[39] Tarazona MP, Boileau S, de Leuze A, Saiz E, Sanchez E, Díaz-Calleja R, Riande E. Conformational and dielectric studies on polysulfides with pyridine groups in the main chain. Macromolecules 1992;25:5020.

[40] Saiz E, Mijangos C, Riande E, López D. Conformational studies on vinyl polymers with sulfur atoms in the side groups. Macromolecules 1994;27:5716.

[41] Flory PJ, Crescenzi V, Mark JE. Configuration of the poly(dimethylsiloxane) chain. III. Correlation of theory and experiment. J Am Chem Soc 1964;86:146.

[42] Mark JE, Flory PJ. Dipole moments of chain molecules. I. Oligomers and polymers of oxyethylene. J Am Chem Soc 1966;88:3702.

[43] Mark JE. Dipole moments of chain molecules. II. Poly(tetramethylene oxide). J Am Chem Soc 1966;88:3708.

[44] Flory PJ, Schimmel PR. Dipole moments in relation to configuration of polypeptide chains. J Am Chem Soc 1967;89:6807.

[45] Mark JE. Dipole moments of dimethylsiloxane chains. J Chem Phys 1968;49:1398.

[46] Mark JE, Ko JH. Configuration-dependent properties of poly(dimethylsilmethylene) chains. II. Correlation of theory and experiment. Macromolecules 1975;8:874.

[47] Tonelli AE. Conformational characteristics of poly(vinylidene fluoride). Macromolecules 1976;9:547.

[48] Abe A. Dipole moments of vinyl polymers with flexible side chains. J Polym Sci, Polym Symp 1976;54:135.

[49] Abe A, Mark JE. Conformational energies and the random-coil dimensions and dipole moments of the polyoxides $CH_3O[(CH_2)_yO]_x$-CH_3. J Am Chem Soc 1976;98:6468.

[50] Abe A. Conformational characteristics of poly(alkyl vinyl ether)'s. Macromolecules 1977;10:34.

[51] Saiz E, Mark JE, Flory PJ. Dipole moments of poly(*p*-chlorostyrene) chains. Macromolecules 1977;10:967.

[52] Mattice WL. Dependence of unperturbed dimensions and dipole moment of poly dialkyl siloxane upon alkyl group length. Macromolecules 1978;11:517.

[53] Abe A, Hirano T, Tsuji K, Tsuruta H. Conformational characteristics of poly[oxy(1-alkylethylenes)] carrying side chains such as ethyl, isopropyl, and *tert*-butyl groups. Macromolecules 1979;12:1100.

[54] Abe A. Configuration-dependent properties of the poly(thioethylene) chain. Macromolecules 1980;13:546.

[55] Abe A, Ando I, Kato K, Uematsu I. Configurational characteristics of poly(oxy-1,1-dimethylethylene). III. Configuration-dependent properties of the polymer chain. Polym J 1981;13:1069.

[56] Abe A, Tasaki K, Mark JE. Rotational isomeric state analysis of poly(oxyethlene). Conformational energies and the random-coil configuration. Polym J 1985;17:883.

[57] Inomata K, Phataralaoha N, Abe A. Conformational characteristics of α,ω-dimethyoxyalkanes and related polymers: a combined use of molecular mechanics calculations and RIS simulations of NMR vicinal coupling constants. Comput Polym Sci 1991;1:126.

[58] Hernandez-Fuentes I, Rey-Stolle F, Tagle LH, Saiz E. Dipole moment of poly(carbonates) with chlorophenyl or dichlorophenyl side groups. Macromolecules 1992;25:3291.

[59] Rathke TD, Frey MW, Guthrie D, Graham R, Simendinger W, Wang BC, Shepard T, Jones R, Tonelli AE. Conformational characteristics of ethylene-vinyl acetate copolymers. Comput Polym Sci 1993;3:61.

[60] Zhou Z, Abe A. Effect of the pendant ester group orientations on the dipole moment of poly(alkyl acrylate)s. Macromolecules 2003;36: 7366.

[61] Zhou Z, Abe A. A RIS treatment of the mean-square dipole moment of PMMA chains in consideration of the pendant ester group orientations. Polymer 2004;45:1313.

[62] Mark JE. Chain dimensions and dipole moments of poly(trimethylene oxide). J Polym Sci, Polym Lett Ed 1966;4:825.

[63] Mark JE. Use of dipole moments to characterize chemical sequence distributions in vinyl copolymers. J Am Chem Soc 1972;94:6645.

[64] Mark JE. Random-coil dimensions and dipole moments of propylene-vinyl chloride copolymers. J Polym Sci, Polym Phys Ed 1973;11: 1375.

[65] Mark JE. Configurational characteristics of ethylene-vinyl chloride copolymers. Polymer 1973;14:553.

[66] Abe A, Hirano T, Tsuruta T. Conformational energies and the random-coil configuration of poly(oxypropylene). Macromolecules 1979;12:1092.

[67] Abe A, Hirano T, Tsuruta T. Conformational characteristics of poly[oxy(1-alkylethylenes)] carrying side chains such as ethyl, isopropyl, and *tert*-butyl groups. Macromolecules 1979;12:1100.

[68] Riande E, Saiz E, Mark JE. Random-coil configurations of the polyformals $[CH_2O(CH_2)_yO]$. 5. Dipole moments, unperturbed dimensions, optical anisotropies, and molar Kerr constants for 1,3-dioxolane polymers containing structural irregularities. Macromolecules 1980;13:448.

[69] Abe A. Conformational analysis of poly(thiopropylene). Macromolecules 1980;13:541.

[70] Tonelli AE. Conformational characteristics of poly(vinyl fluoride), poly(fluoromethylene), and poly(trifluoroethylene). Macromolecules 1980;13:734.

[71] Tonelli AE. Conformational characteristics of poly(vinyl bromide) and ethylene-vinyl bromide copolymers. Macromolecules 1982;15: 290.

[72] Riande E, Mark JE. Dipole moments of some poly(dimethylsiloxane) linear chains and cyclics. Eur Polym J 1984;20:517.

[73] Wang S, Mark JE. Conformational and configurational analysis of linear poly(ethylene imine). Comput Polym Sci 1993;3:79.

[74] Mattice WL, Helfer CA, Sokolov AP. Persistence length and the finite chain length effect on characteristic ratios. Macromolecules 2004;37:4711.

[75] Flory PJ. Foundations of rotational isomeric state theory and general methods for generating configurational average. Macromolecules 1974;7:381.

[76] Mattice WL, Helfer CA, Sokolov AP. On the relationship between the characteristic ratio of a finite chain, C_n, and the asymptotic limit, C_α. Macromolecules 2003;36:10071.